

On the Interface between Perturbative and Nonperturbative QCD

Alexandre Deur

*Thomas Jefferson National Accelerator Facility, Newport News, VA 23606, USA*¹

Stanley J. Brodsky

*SLAC National Accelerator Laboratory, Stanford University, Stanford, CA 94309, USA*²

Guy F. de Téramond

*Universidad de Costa Rica, 11501 San Pedro de Montes de Oca, Costa Rica*³

Abstract

The QCD running coupling $\alpha_s(Q^2)$ sets the strength of the interactions of quarks and gluons as a function of the momentum transfer Q . The Q^2 dependence of the coupling is required to describe hadronic interactions at both large and short distances. In this article we adopt the light-front holographic approach to strongly-coupled QCD, a formalism which incorporates confinement, predicts the spectroscopy of hadrons composed of light quarks, and describes the low- Q^2 analytic behavior of the strong coupling $\alpha_s(Q^2)$. The high- Q^2 dependence of the coupling $\alpha_s(Q^2)$ is specified by perturbative QCD and its renormalization group equation. The matching of the high and low Q^2 regimes of $\alpha_s(Q^2)$ then determines the scale Q_0 which sets the interface between perturbative and nonperturbative hadron dynamics. The value of Q_0 can be used to set the factorization scale for DGLAP evolution of hadronic structure functions and the ERBL evolution of distribution amplitudes. We discuss the scheme-dependence of the value of Q_0 and the infrared fixed-point of the QCD coupling. Our analysis is carried out for the \overline{MS} , g_1 , MOM and V renormalization schemes. Our results show that the discrepancies on the value of α_s at large distance seen in the literature can be explained by different choices of renormalization schemes. We also provide the formulae to compute $\alpha_s(Q^2)$ over the entire range of space-like momentum transfer for the different renormalization schemes discussed in this article.

¹deurpam@jlab.org

²sjbth@slac.stanford.edu

³gdt@asterix.crnet.cr

Contents

1	Introduction	2
2	Holographic mapping and matching procedure	5
3	Results	7
4	Conclusions	10

1 Introduction

The behavior of the QCD coupling $\alpha_s(Q^2)$ at low momentum transfer Q is a central field of study in hadron physics. Key questions are the analytic behavior of the coupling in the infrared (IR), such as whether it exhibits a nonzero IR fixed point and whether it displays conformal-like behavior at low momentum transfers. Different theoretical approaches to QCD dynamics, such as lattice gauge theory, Schwinger-Dyson equations and light-front holographic methods use different definitions of the QCD coupling and effective charges to study $\alpha_s(Q^2)$ in the IR domain [1, 2].

Knowing the strength of the strong coupling α_s in the nonperturbative domain is necessary for understanding fundamental problems in hadron physics, including the mechanisms for color confinement and the origin of gluonic flux tubes within hadrons. The magnitude of the coupling at low momentum even has impact on high energy phenomena, such as the amplitude for heavy-quark pair production near threshold [3] and the magnitude of the T -odd Sivers effects in semi-inclusive polarized deep inelastic scattering [4].

There is, however, no consensus on the IR behavior of $\alpha_s(Q^2)$. The diversity of possible behaviors can be partly traced back to the different definitions of α_s in the nonperturbative domain. For example, one can define the QCD coupling as an “effective charge” from any perturbatively calculable observable [5]. The various choices for the coupling typically differ from the standard perturbative definition, such as $\alpha_{\overline{MS}}$, due to the inclusion of nonperturbative contributions which eliminate an unphysical Landau pole in the physical domain. Indeed, the inclusion of the nonperturbative contributions leads to a modification of the behavior of the coupling in the IR domain.

Studies which simulate a linear confining potential suggest that $\alpha_s(Q^2)$ diverges as $1/Q^2$ for $Q^2 \rightarrow 0$ [6, 7]. However, this identification is ambiguous, since the linear

confining potential for nonrelativistic heavy quarks in the usual instant form of dynamics [8] is equivalent, at large separation distances, to a harmonic oscillator potential in the light-front (LF) form of relativistic dynamics [8, 9]. Furthermore, it should be noted that unlike QED, the QCD potential cannot be uniquely identified with single gluon exchange. Other approaches suggest that $\alpha_s(Q^2)$ vanishes as $Q^2 \rightarrow 0$ [10].

In this paper we shall consider the case where $\alpha_s(Q^2)$ becomes constant at low Q^2 [11, 12, 13, 14]. This behavior, called the “freezing” of the coupling to a fixed IR value, is automatic if one defines the coupling from an effective charge, and it is thus appealing from physical considerations [11, 15]. On simple terms, confinement implies that long wavelengths of quarks and gluons are cutoff at a typical hadronic size. Consequently, the effects of quantum loops responsible for the logarithmic dependence of α_s vanish and α_s should freeze to a constant value at hadronic scales [16, 17]. There are considerable variations in the literature on what should be the freezing value of the strong coupling – it typically ranges from 0.6 to π [1]. As noted in Ref. [11], the choice of renormalization scheme (RS) can explain an important part of the spread in the freezing values reported in the literature. As we shall show here, an explicit connection between the large-distance confining dynamics of hadronic physics and the short-distance dynamics of quarks and gluons [18] allows one to quantitatively determine this dependence in any RS.

We shall use here the light-front holographic approach to nonperturbative infrared dynamics [19]. This innovative approach to color confinement allows us to determine the behavior of the strong coupling in the IR domain [11]. Using this framework, one can show that the first-order semiclassical approximation to the light-front QCD Hamiltonian is formally equivalent to the eigenvalue equations in anti-de Sitter (AdS) space [20, 21]. This connection also provides a precise relation between the holographic variable z of AdS_5 space and the light-front variable ζ [20, 22]. For a two-particle bound state the invariant distance squared between the quark and antiquark in the light-front wavefunction of a meson is defined as $\zeta^2 = x(1-x)b_\perp^2$, where $x = k^+/P^+$ is the quark’s light-front momentum fraction, and b_\perp is the transverse separation between the q and \bar{q} . It is also conjugate to the invariant mass $k_\perp^2/x(1-x)$ of the $q\bar{q}$ system.

Light-front holography provides a unification of both light-front kinematics and dynamics: the non-trivial geometry of AdS space encodes the kinematical aspects, and the deformation of the action in AdS_5 space – described in terms of a specific dilaton profile $e^{+\kappa^2 z^2}$, encompasses confinement dynamics and determines the effective potential $\kappa^4 \zeta^2$ in the light-front Hamiltonian [21]. The eigenvalues of the resulting light-front

Hamiltonian predict the Regge spectrum of the hadrons, consistent with experiments, and its eigenfunctions determine the light-front wavefunctions underlying form factors, structure functions and other properties of hadrons. The value of the mass parameter κ can be determined from a single hadronic input, such as the proton mass: $\kappa = m_p/2$.

A further advantage of the light-front holographic mapping is that one can determine the analytic behavior of the strong coupling in the IR: It has the form $\alpha_s(Q^2) \propto \exp(-Q^2/4\kappa^2)$. This prediction follows from the IR modification of AdS space, *i.e.*, from the same dilaton profile which predicts the Regge spectrum [11, 19]. As we have shown in Ref. [11], this form gives a remarkable description of the effective charge $\alpha_{g1}(Q^2)$ determined from measurements of the g_1 polarized structure function of the nucleon [23, 24].

One can also show that the analytic dependence of the confinement potential is uniquely determined by enforcing conformal symmetry –an exact symmetry of the QCD classical Lagrangian when quark masses are neglected. This method, originally discussed by de Alfaro, Fubini and Furlan (dAFF) in the context of one-dimensional quantum field theory allows one to determine uniquely the confinement potential in bound-state equations while keeping the action conformally invariant [25]. One can extend the conformal quantum mechanics of dAFF to 3+1 physical space-time on the light front [26]. The resulting confinement potential is the transverse harmonic oscillator $\kappa^4 \zeta^2$ in the light-front Hamiltonian which successfully describes hadronic spectra and form factors [19]. Conversely, LF holography determines the AdS₅ dilaton profile $e^{+\kappa^2 z^2}$ and thus the analytic dependence $\alpha_s(Q^2) \propto \exp(-Q^2/4\kappa^2)$ of the strong coupling in the IR.

This view has received recently strong support from superconformal quantum mechanics [27, 28] and its extension to light-front physics [29, 30]. This new approach to hadron physics captures very well the essential physics of QCD confining dynamics and gives remarkable connections between the baryon and meson spectra. Furthermore, it gives remarkable connections across the full heavy-light hadron spectra, where heavy quark masses break the conformal invariance, but the underlying supersymmetry still holds [31]. In this framework, the emergent dynamical supersymmetry is not a consequence of supersymmetric QCD, at the level of fundamental fields, but relies on the fact that in $SU(3)_C$ a diquark can be in the same color representation as an antiquark, namely a $\bar{\mathbf{3}} \sim \mathbf{3} \times \mathbf{3}$.

We shall show in this paper how the holographic procedure can be extended to describe the strong coupling in the nonperturbative and perturbative domains for any choice of effective charge and RS. The large momentum-transfer dependence of the cou-

pling $\alpha_s(Q^2)$ is specified by perturbative QCD (pQCD) and its renormalization group equation. The matching of the high and low momentum transfer regimes of $\alpha_s(Q^2)$ determines the scale Q_0 which sets the interface between the perturbative and nonperturbative regimes. Since the value of Q_0 determines the starting point for pQCD, it can be used to set the factorization scale for DGLAP evolution of hadronic structure functions [32] and the ERBL evolution of distribution amplitudes [33]. We will also discuss the dependence of Q_0 on the choice of the effective charge used to define the running coupling and the RS used to compute its behavior in the perturbative regime. Our analysis also determines the infrared fixed-point behavior of the QCD coupling as well as the value of the infrared fixed point, $\alpha_s(0)$, for any choice of effective charge and RS.

2 Holographic mapping and matching procedure

The QCD coupling α_s can be defined as an “effective charge” [5] satisfying the standard renormalization group evolution equation. This is analogous to the definition of the QED coupling from the potential between heavy leptons by Gell Mann and Low [34]. As we shall show in this section, the analytic behavior of the running coupling α_s in the low- Q^2 nonperturbative domain [11] can be uniquely predicted using the light-front holographic approach to strongly coupled QCD [19]. It can then be matched [18] to form the running coupling at large Q^2 as predicted by perturbative QCD in any RS.

The low Q^2 -evolution of α_s is derived from the long-range confining forces: the originally constant, *i.e.* the conformal invariant light-front holographic (LFH) coupling $\alpha_s^{LFH} \equiv g_{LFH}^2/4\pi$, is redefined to include the effects of QCD’s long-range confining force. As we shall show in detail, the Q^2 dependence of the coupling in the IR follows from the specific embedding of light-front dynamics in AdS space [11]; it is uniquely determined in terms of the dilaton profile originating from the specific breaking of conformal invariance consistent with the dAFF mechanism [25, 26]. Likewise, the coupling at short distances, as described by perturbative QCD, becomes Q^2 -dependent because short-distance QCD quantum effects are included in its definition.

We start with the dilaton modified AdS₅ action:

$$S_{AdS} = -\frac{1}{4} \int d^4x dz \sqrt{|g|} e^{\varphi(z)} \frac{1}{g_{AdS}^2} F^2, \quad (1)$$

where g is the AdS metric determinant, g_{AdS} the AdS coupling, and the dilaton profile is

given by $\varphi = \kappa^2 z^2$. The scale κ controls quark confinement and determines the hadron masses in LF holographic QCD [19]. It also determines the Q^2 dependence of the strong coupling from the large-distance confining forces, *i.e.* the effect of the modification of the AdS space curvature from nonconformal confinement dynamics [11]:

$$g_{AdS}^2 \rightarrow g_{AdS}^2 e^{-\kappa^2 z^2}. \quad (2)$$

The five-dimensional coupling $g_{AdS}(z)$ is mapped, modulo a constant, to the LFH coupling $g_{LFH}(\zeta)$ of the confining theory in physical space-time. The holographic variable z is identified with the physical invariant impact separation variable ζ [20, 22]:

$$g_{AdS}(z) \rightarrow g_{LFH}(\zeta). \quad (3)$$

We thus have

$$\alpha_s^{LFH}(\zeta) \equiv \frac{g_{LFH}^2(\zeta)}{4\pi} \propto e^{-\kappa^2 \zeta^2}. \quad (4)$$

The physical coupling measured at space-like 4-momentum squared $Q^2 = -q^2$ is the light-front transverse Fourier transform of the LFH coupling $\alpha_s^{LFH}(\zeta)$ (4):

$$\alpha_s^{LFH}(Q^2) \sim \int_0^\infty \zeta d\zeta J_0(\zeta Q) \alpha_s^{LFH}(\zeta), \quad (5)$$

in the $q^+ = 0$ light-front frame where $Q^2 = -q^2 = -\mathbf{q}_\perp^2 > 0$, and J_0 is a Bessel function. Using this ansatz we then have from Eq. (5)

$$\alpha_s^{LFH}(Q^2) = \alpha_s^{LFH}(0) e^{-Q^2/4\kappa^2}. \quad (6)$$

The effective charge $\alpha_{g_1} = g_1^2/4\pi$ is defined from the integral appearing in the Bjorken sum rule [23, 24]

$$\frac{\alpha_{g_1}(Q^2)}{\pi} = 1 - \frac{6}{g_A} \int_0^{1^-} dx g_1^{p-n}(x, Q^2), \quad (7)$$

where $x = x_{Bj}$ is the Bjorken scaling variable, g_1^{p-n} is the isovector component of the nucleon spin structure function, and g_A is the nucleon axial charge. The IR fixed-point of α_{g_1} is kinematically constrained to the value $\alpha_{g_1}(0)/\pi = 1$. However, we will ignore this constraint here since one of our goals is to determine the freezing value of $\alpha_s(0)$ for different RS from the matching procedure described below. An agreement with the value $\alpha_s(0)/\pi = 1$ for the g_1 -effective charge will demonstrate the consistency of the

procedure.

Eq. (6) is valid only in the nonperturbative regime. However, it can be continued to the pQCD domain thanks to an overlap existing between the pQCD and nonperturbative QCD regimes known as parton-hadron duality [35, 36]. The nonperturbative coupling, Eq. (6), and its β function, $\beta(Q^2) = d\alpha_s(Q^2)/d\log(Q^2)$, can be equated to their pQCD counterparts for each RS considered here. Thus, we shall impose the conditions $\alpha_s^{pQCD}(Q_0^2) = \alpha_s^{LFH}(Q_0^2)$ and $\beta^{pQCD}(Q_0^2) = \beta^{LFH}(Q_0^2)$, where the transition scale Q_0^2 indicates the onset of the pQCD regime as obtained from the matching procedure. The solution of this system of equations is unique, providing a relation between a nonperturbative quantity, such as κ or $\alpha_s(0)$, and the fundamental QCD scale Λ in a given RS. It also sets the value of Q_0^2 . This matching procedure was used in Ref. [18] to determine the QCD scale in the \overline{MS} scheme, $\Lambda_{\overline{MS}}$. It is found that $\Lambda_{\overline{MS}} = 0.341 \pm 0.032$ GeV, in remarkable agreement with the combined world data $\Lambda_{\overline{MS}}^{(3)} = 0.340 \pm 0.008$ GeV [37] and the latest lattice calculations [38]. In this article, we will use the known values of Λ in several RS to obtain the corresponding values of $\alpha_s(0)$ and Q_0 .

3 Results

In this section we shall derive the form of $\alpha_s^{LFH}(Q^2)$ for effective charges assuming the value $\kappa = 0.51 \pm 0.04$ GeV. The value of the RS-independent scale κ is obtained by averaging the predictions of light-front holography for the ρ -meson mass, $\kappa = M_\rho/\sqrt{2}$, and the nucleon mass, $\kappa = M_N/2$ [19]. The scale κ can also be extracted from other observables, including hadron masses [19], an extension of the holographic model to describe hadron form factors [19], and the low Q^2 dependence of the Bjorken integral [11, 18]. For example, the determination of κ from the measurements of the Bjorken integral yields the value $\kappa = 0.513 \pm 0.007$ GeV. The ± 0.04 variation covers the possible values of κ and is characteristic of the uncertainties associated with the approximations to strongly coupled QCD using the LFH approach. The RS-dependent freezing value $\alpha_s(0)$ will be left as a free parameter.

We shall use the perturbative coupling $\alpha_s^{pQCD}(Q^2)$ calculated up to order β_3 in the perturbative series of the β function

$$Q^2 \frac{\partial \alpha_s}{\partial Q^2} = \beta(\alpha_s) = - \left(\frac{\alpha_s}{4\pi} \right)^2 \sum_{n=0} \left(\frac{\alpha_s}{4\pi} \right)^n \beta_n. \quad (8)$$

We take the number of quark flavors $n_f = 3$, and the values of the QCD scale Λ in each

scheme as determined at large Q^2 ; see Table 1. The matching procedure then allows us to establish the IR-behavior of α_s in any RS.

An approximate analytical expression valid up to order β_3 can be obtained by iteration [39]:

$$\begin{aligned} \alpha_s^{pQCD}(Q^2) = & \frac{4\pi}{\beta_0 \ln(Q^2/\Lambda^2)} \left[1 - \frac{\beta_1}{\beta_0^2} \frac{\ln[\ln(Q^2/\Lambda^2)]}{\ln(Q^2/\Lambda^2)} \right. \\ & + \frac{\beta_1^2}{\beta_0^4 \ln^2(Q^2/\Lambda^2)} \left((\ln[\ln(Q^2/\Lambda^2)])^2 - \ln[\ln(Q^2/\Lambda^2)] - 1 + \frac{\beta_2 \beta_0}{\beta_1^2} \right) \\ & + \frac{\beta_1^3}{\beta_0^6 \ln^3(Q^2/\Lambda^2)} \left(-(\ln[\ln(Q^2/\Lambda^2)])^3 + \frac{5}{2} (\ln[\ln(Q^2/\Lambda^2)])^2 \right. \\ & \left. \left. + 2 \ln[\ln(Q^2/\Lambda^2)] - \frac{1}{2} - 3 \frac{\beta_2 \beta_0}{\beta_1^2} \ln[\ln(Q^2/\Lambda^2)] + \frac{\beta_3 \beta_0^2}{2 \beta_1^3} \right) \right]. \quad (9) \end{aligned}$$

This result is valid in the \overline{MS} (minimal-subtraction), V (potential) and MOM (momentum-subtraction) schemes [37].

The first two coefficients of the β series

$$\beta_0 = 11 - \frac{2}{3} n_f, \quad (10)$$

and

$$\beta_1 = 102 - \frac{38}{3} n_f, \quad (11)$$

are scheme independent. The higher order coefficients for the \overline{MS} renormalization scheme are [40]

$$\beta_2 = \frac{2857}{2} - \frac{5033}{18} n_f + \frac{325}{54} n_f^2, \quad (12)$$

and

$$\begin{aligned} \beta_3 = & \left(\frac{149753}{6} + 3564 \xi(3) \right) - \left(\frac{1078361}{162} + \frac{6508}{27} \xi(3) \right) n_f + \left(\frac{50065}{162} + \frac{6472}{81} \xi(3) \right) n_f^2 \\ & + \frac{1093}{729} n_f^3, \quad (13) \end{aligned}$$

with the Apéry constant $\xi(3) \simeq 1.20206$. In the MOM scheme and Landau gauge, the coefficients are [41]

$$\beta_2 = 3040.48 - 625.387 n_f + 19.3833 n_f^2, \quad (14)$$

and

$$\beta_3 = 100541 - 24423.3n_f + 1625.4n_f^2 - 27.493n_f^3. \quad (15)$$

Four-loop calculations are also available in the related *minimalMOM* scheme [42]. In the V scheme the coefficients are [43]

$$\beta_2 = 4224.181 - 746.0062n_f + 20.87191n_f^2, \quad (16)$$

and

$$\beta_3 = 43175.06 - 12951.7n_f + 706.9658n_f^2 - 4.87214n_f^3. \quad (17)$$

Finally, in the g_1 scheme/effective charge, the perturbative coupling expression is [24]:

$$\alpha_{g_1}(Q^2) = \alpha_{\overline{MS}} + 3.58 \frac{\alpha_{\overline{MS}}^2}{\pi} + 20.21 \frac{\alpha_{\overline{MS}}^3}{\pi^2} + 175.7 \frac{\alpha_{\overline{MS}}^4}{\pi^3}. \quad (18)$$

The β -series order for the $\alpha_{\overline{MS}}$ expression in Eq. (18) is typically taken to be the same as the $\alpha_{\overline{MS}}$ order of Eq. (18); this is 4th order in the present case.

We have carried out the matching procedure numerically for the \overline{MS} , V , MOM (choosing the Landau gauge) and the g_1 schemes. Our results are presented in Figs. 1, 2 and 3. In Fig. 1, we show $\alpha_s(0)$ as a function of Q_0^2 for the first matching condition $\alpha_s^{pQCD}(Q_0^2) = \alpha_s^{LFH}(Q_0^2)$. The two curves illustrated for each scheme represent the results when the matching is done with α_s^{pQCD} calculated either at order β_2 or β_3 . For the g_1 scheme, the expression of $\alpha_{g_1}^{pQCD}$ is a series in $\alpha_{\overline{MS}}^{pQCD}$ rather than in β_i , see Eq. (18). In that case the calculations are done at fourth order in $\alpha_{\overline{MS}}^{pQCD}$ calculated at β_2 or β_3 .

The second matching condition requires the continuity of the β -function, $\beta^{pQCD}(Q_0^2) = \beta^{LFH}(Q_0^2)$. The solution is given by the extrema of the curves. The two matching conditions provide the values of $\alpha_s(0)$ and Q_0^2 . The corresponding couplings are shown in Fig. 2. A comparison between data and our result for $\alpha_{g_1}(Q^2)$ is shown on Fig. 3.

The difference between the results obtained with α_s^{pQCD} calculated at order β_2 or at order β_3 provide an estimate of the uncertainty due to the series truncation. Other contributions (not shown in the figures) come from the uncertainties in the values of κ and Λ . For the latter, we have assumed a 5% relative uncertainty.

The different freezing values and Q_0^2 scales obtained are listed in Table 1. Our results for $\alpha_s(0)$ can be compared to the typical values from the literature. Most of the results from Lattice QCD, the Schwinger-Dyson formalism, stochastic quantization and the functional renormalization group equations are carried out in the MOM scheme and Landau gauge for $n_f = 0$ [1]. These computations yield $\alpha_s(0) = 2.97$ [1], which can be

$\alpha_s(0)$	RS	Q_0^2 (GeV)	Λ (GeV)
$1.22 \pm 0.04 \pm 0.11 \pm 0.09$	\overline{MS}	$0.75 \pm 0.03 \pm 0.05 \pm 0.04$	0.34 ± 0.02
$2.30 \pm 0.03 \pm 0.28 \pm 0.21$	V	$1.00 \pm 0.00 \pm 0.07 \pm 0.06$	0.37 ± 0.02
$3.79 \pm 0.06 \pm 0.65 \pm 0.46$	MOM	$1.32 \pm 0.02 \pm 0.10 \pm 0.08$	0.52 ± 0.03
$3.51 \pm 0.14 \pm 0.49 \pm 0.35$	g_1	$1.14 \pm 0.04 \pm 0.08 \pm 0.06$	0.92 ± 0.05

Table 1: Freezing values for α_s (column 1) calculated in different schemes (column 2) and for $n_f = 3$. The scale of the pQCD onset is given in the third column. The RS-dependent values of Λ are in the fourth column. The first, second and third uncertainties on $\alpha_s(0)$ and Q_0^2 stem from the truncation of the β -series determining α_s^{pQCD} , the ± 0.04 GeV uncertainty on κ and the 5% uncertainty on Λ , respectively.

compared with $\alpha_s(0) = 2.84$ obtained using our procedure with $n_f = 0$. The result from Cornwall [44] using $n_f = 3$ and in the \overline{MS} scheme yields $\alpha_s(0) = 0.91$ [1], in agreement with our \overline{MS} determination. The constraint $\alpha_s(0) = \pi$ in the g_1 scheme also agrees well with our analysis.

The scheme dependence of the freezing value is easily understood by considering the slope of α_s near Q_0^2 , which depends on the scheme-dependent value of Λ : the steeper the slope, the larger $\alpha_s(0)$. The scheme dependence of the transition scale Q_0^2 is likewise easily explained: the smaller the freezing value, the earlier the onset of pQCD. Our Q_0^2 values are close to the value found in Ref. [13] where, in order to explain parton-hadron duality, the evolution of $\alpha_{\overline{MS}}^{pQCD}(Q^2)$ near $Q_0^2 \simeq 1$ GeV² is stopped. It is also consistent with the transition value $Q_0^2 = 0.87$ GeV² found in Ref. [45] using the \overline{MS} scheme.

The full Q^2 dependence of $\alpha_s(Q^2)$ for a specific RS can be conveniently represented in the form

$$\alpha_s(Q^2) = \alpha_s(0) e^{\frac{-Q^2}{4\kappa^2}} H(Q^2 - Q_0^2) + (1 - H(Q^2 - Q_0^2)) \alpha_s^{pQCD}(Q^2), \quad (19)$$

where $\kappa = 0.51 \pm 0.04$ GeV, $H(Q^2)$ is the Heaviside step function, α_s^{pQCD} is given by Eq. 9 for the \overline{MS} , MOM or V schemes or by Eq. (18) for the g_1 scheme, and $\alpha_s(0)$ and Q_0^2 are given in Table 1.

4 Conclusions

The dependence of the freezing value of $\alpha_s(Q^2)$ at low Q^2 on the choice of the effective charge and the pQCD renormalization scheme can be quantitatively estimated using the light-front holographic approach to strongly coupled QCD and the matching procedure

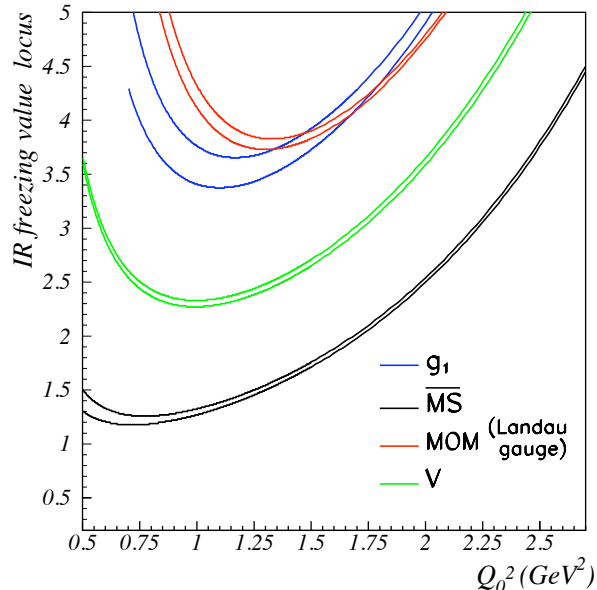


Figure 1: The freezing value $\alpha_s(0)$ versus the transition scale Q_0^2 . Calculations are done in \overline{MS} scheme (black lines), the g_1 scheme (blue lines), the V scheme (green lines) and the MOM scheme (red lines). Two lines of same color represent results obtained with α_s^{pQCD} calculated either at order β_2 or β_3 . The extrema of these curves provide the value of Q_0^2 and $\alpha_s(0)$ that meets the matching conditions $\alpha_s^{pQCD}(Q_0^2) = \alpha_s^{LFH}(Q_0^2)$ and $\beta^{pQCD}(Q_0^2) = \beta^{LFH}(Q_0^2)$.

described in Ref. [18]. The results we have obtained in this paper for $\alpha_s(Q^2 = 0)$ in the deep infrared, ranging from 0.98 to 4.96, show that the choice of renormalization scheme and the choice of the effective charge used to define the QCD coupling strongly influences its freezing value. For example, the freezing values reported in the literature typically range from ~ 0.6 to ~ 3 : accounting for the scheme/effective charge dependence thus resolves a large part of this discrepancy. In fact, our values of $\alpha_s(0)$ for the \overline{MS} , MOM and g_1 schemes agree with the corresponding typical values encountered in the literature.

Other factors must also be considered before comparing various couplings proposed in the literature, including which approximations are used. For example, many calculations in the MOM scheme are done without dynamical quarks. If one takes $n_f = 0$ we find a central value $\alpha_s(0) = 2.84$ in the MOM scheme, in comparison with $\alpha_s(0) = 3.79$ for $n_f = 3$. Another factor is the choice of gauge for gauge-dependent definitions of $\alpha_s(Q^2)$, such as the ones defined from vertices and propagators [1] or the definition using the gluon self-energy and the pinch technique [12, 46]. It was however shown that an appropriately chosen gauge can lead to similar behavior between the pinched defined coupling and the one defined from the ghost-gluon vertex [47]. This was demonstrated

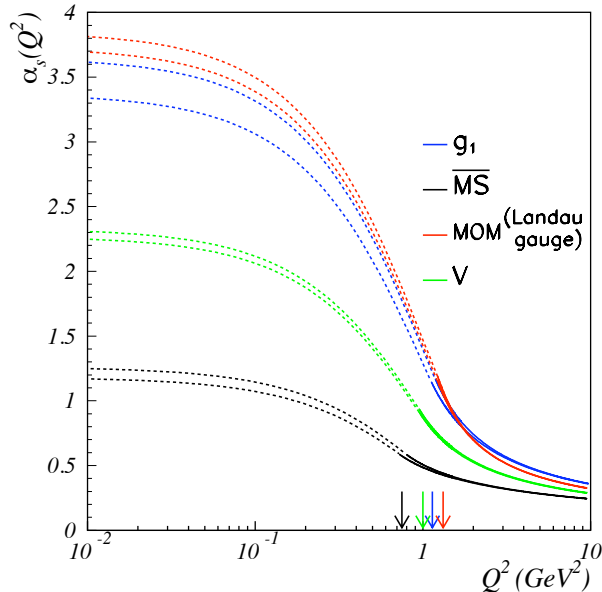


Figure 2: The strong coupling $\alpha_s(Q^2)$ for different schemes. The continuous lines are the perturbative calculations done either at order β_2 or β_3 . The dashed curves are their matched continuations into the non-perturbative domain. The location of the scale Q_0^2 for the transition from the nonperturbative to the perturbative region is shown by the arrows for each scheme.

in the Landau gauge and the *MOM* scheme. Different couplings can be defined from other vertices and propagators, but they are related to the ghost-gluon vertex coupling. These relations have been discussed in Ref. [48] for the *MOM* scheme.

As we have shown, matching the high and low momentum transfer regimes of the running QCD coupling, as determined from light-front holographic QCD and pQCD evolution, determines the scale Q_0 which sets the interface between perturbative and nonperturbative hadron dynamics. Above Q_0 , the perturbative gluon and quark degrees of freedom are relevant. Below Q_0 , the collective effects of the gluonic interactions can be understood to provide the potential $\kappa^4 \zeta^2$ in the effective LF Hamiltonian underlying light quark meson and baryon spectroscopy. In addition, the collective gluonic effects can provide the basis for phenomena such as the “flux tubes” [49, 50], which are postulated to connect the incident quark and diquarks in high energy hadronic collisions.

The specific numerical value for the transition scale Q_0 is also important for hadron physics phenomenology. The value of Q_0 can be understood as the starting point for pQCD evolution from gluonic radiation; it thus can be used to set the factorization scale for DGLAP evolution of hadronic structure functions [32] and the ERBL evolution of distribution amplitudes [33].

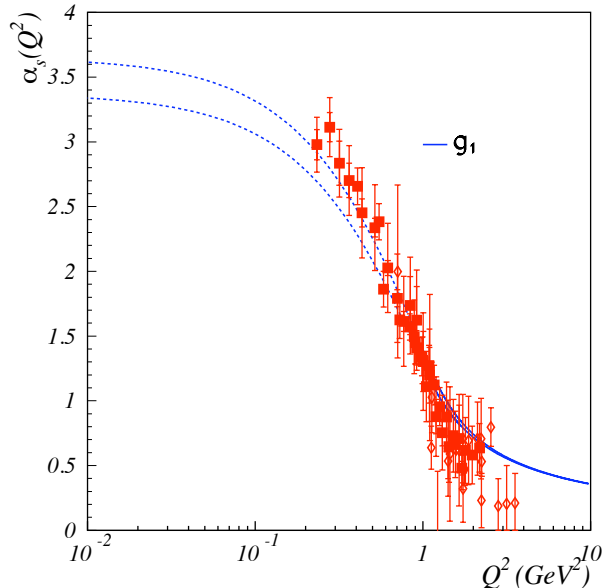


Figure 3: Comparison between the experimental data [24] and the prediction from our matching procedure and the value of Λ listed in Table 1. The coupling is calculated in the g_1 scheme. The inner error bar on each experimental data point is the point-to-point uncorrelated uncertainty and the outer error bar represents the total uncertainty (point-to-point correlated and uncorrelated uncertainties added in quadrature).

The use of the transition scale Q_0 to eliminate the factorization scale uncertainty, in combination with the “principle of maximum conformality” (PMC) [51], which sets renormalization scales order by order to obtain scheme-independent pQCD predictions for observables, can eliminate important theoretical uncertainties and thus greatly improve the precision of pQCD predictions for collider phenomenology.

Acknowledgments

This material is based upon work supported by the U.S. Department of Energy, Office of Science, Office of Nuclear Physics under contract DE-AC05-06OR23177. This work is also supported by the Department of Energy contract DE-AC02-76SF00515. SLAC-PUB-16449.

References

- [1] For a recent review see, A. Deur, S. J. Brodsky, G. F. de Teramond, The QCD running coupling (JLAB-PHY-16-2199, SLAC-PUB-16448, to be published in Prog. Nuc. Part. Phys. (2016)) and references within.
- [2] G. M. Prosperi, M. Raciti and C. Simolo, On the running coupling constant in QCD, *Prog. Part. Nucl. Phys.* **58**, 387 (2007) [[arXiv:hep-ph/0607209](#)].
- [3] S. J. Brodsky, A. H. Hoang, J. H. Kuhn and T. Teubner, Angular distributions of massive quarks and leptons close to threshold, *Phys. Lett. B* **359**, 355 (1995) [[arXiv:hep-ph/9508274](#)].
- [4] S. J. Brodsky, D. S. Hwang and I. Schmidt, Final-state interactions and single-spin asymmetries in semi-inclusive deep inelastic scattering, *Phys. Lett. B* **530**, 99 (2002) [[arXiv:hep-ph/0201296](#)].
- [5] G. Grunberg, Renormalization group improved perturbative QCD, *Phys. Lett. B* **95**, 70 (1980); Renormalization scheme independent QCD and QED: The method of effective charges, *Phys. Rev. D* **29**, 2315 (1984); On some ambiguities in the method of effective charges, *Phys. Rev. D* **40**, 680 (1989).
- [6] J. L. Richardson, The heavy quark potential and the Υ , J/ψ systems, *Phys. Lett. B* **82**, 272 (1979).
- [7] See *e.g.*, A. V. Nesterenko, Quark-antiquark potential in the analytic approach to QCD, *Phys. Rev. D* **62**, 094028 (2000) [[arXiv:hep-ph/9912351](#)]; R. Alkofer, C. S. Fischer and F. J. Llanes-Estrada, Dynamically induced scalar quark confinement, *Mod. Phys. Lett. A* **23**, 1105 (2008) [[arXiv:hep-ph/0607293](#)]; Y. O. Belyakova and A. V. Nesterenko, A nonperturbative model for the strong running coupling within potential approach, *Int. J. Mod. Phys. A* **26**, 981 (2011) [[arXiv:1011.1148 \[hep-ph\]](#)]; see [1] for an exhaustive list of references.
- [8] P. A. M. Dirac, Forms of relativistic dynamics, *Rev. Mod. Phys.* **21**, 392 (1949).
- [9] A. P. Trawiński, S. D. Glazek, S. J. Brodsky, G. F. de Teramond and H. G. Dosch, Effective confining potentials for QCD, *Phys. Rev. D* **90**, 074017 (2014) [[arXiv:1403.5651 \[hep-ph\]](#)].

- [10] P. Boucaud, J. P. Leroy, A. L. Yaouanc, J. Micheli, O. Pene and J. Rodriguez-Quintero, IR finiteness of the ghost dressing function from numerical resolution of the ghost SD equation, *JHEP* **0806**, 012 (2008) [[arXiv:0801.2721 \[hep-ph\]](#)]; On the IR behaviour of the Landau-gauge ghost propagator, *JHEP* **0806**, 099 (2008) [[arXiv:0803.2161 \[hep-ph\]](#)]; J. C. R. Bloch, A. Cucchieri, K. Langfeld and T. Mendes, Running coupling constant and propagators in SU(2) Landau gauge, *Nucl. Phys. Proc. Suppl.* **119**, 736 (2003) [[arXiv:hep-lat/0209040](#)]; A. C. Aguilar and A. A. Natale, A Dynamical gluon mass solution in a coupled system of the Schwinger-Dyson equations, *JHEP* **0408**, 057 (2004) [[arXiv:hep-ph/0408254](#)]; C. Kellermann and C. S. Fischer, The Running coupling from the four-gluon vertex in Landau gauge Yang-Mills theory, *Phys. Rev. D* **78**, 025015 (2008) [[arXiv:0801.2697 \[hep-ph\]](#)]; see [1] for an exhaustive list of references.
- [11] S. J. Brodsky, G. F. de Teramond and A. Deur, Nonperturbative QCD coupling and its β -function from light-front holography, *Phys. Rev. D* **81**, 096010 (2010) [[arXiv:1002.3948 \[hep-ph\]](#)].
- [12] J. M. Cornwall, Dynamical mass generation in continuum QCD, *Phys. Rev. D* **26**, 1453 (1982).
- [13] A. Courtoy, S. Liuti, Extraction of α_s from deep inelastic scattering at large x , *Phys. Lett. B* **726**, 320 (2013) [[arXiv:1302.4439 \[hep-ph\]](#)].
- [14] A. C. Aguilar, A. Mihara and A. A. Natale, Freezing of the QCD coupling constant and solutions of Schwinger-Dyson equations, *Phys. Rev. D* **65**, 054011 (2002) [[arXiv:hep-ph/0109223](#)]; A. V. Nesterenko and J. Papavassiliou, The massive analytic invariant charge in QCD, *Phys. Rev. D* **71**, 016009 (2005) [[arXiv:hep-ph/0410406](#)]; J. A. Gracey, One loop gluon form factor and freezing of α_s in the Gribov-Zwanziger QCD Lagrangian, *JHEP* **0605**, 052 (2006) [[arXiv:hep-ph/0605077](#)]; A. Ayala, A. Bashir, D. Binosi, M. Cristoforetti and J. Rodriguez-Quintero, Quark flavor effects on gluon and ghost propagators, *Phys. Rev. D* **86**, 074512 (2012) [[arXiv:1208.0795 \[hep-ph\]](#)]; see [1] for an exhaustive list of references.
- [15] C. S. Fischer and J. M. Pawłowski, Uniqueness of infrared asymptotics in Landau gauge Yang-Mills theory, *Phys. Rev. D* **75** (2007) 025012 [[arXiv:hep-th/0609009](#)]; Uniqueness of infrared asymptotics in Landau gauge Yang-Mills theory II, *Phys. Rev. D* **80**, 025023 (2009) [[arXiv:0903.2193 \[hep-th\]](#)]; C. S. Fischer, A. Maas

- and J. M. Pawłowski, On the infrared behavior of Landau gauge Yang-Mills theory, *Annals Phys.* **324**, 2408 (2009) [[arXiv:0810.1987](#) [[hep-ph](#)]].
- [16] S. J. Brodsky and G. F. de Teramond, Light-front dynamics and AdS/QCD correspondence: the pion form factor in the space- and time-like regions, *Phys. Rev. D* **77**, 056007 (2008) [[arXiv:0707.3859](#) [[hep-ph](#)]].
- [17] S. J. Brodsky and R. Shrock, Maximum wavelength of confined quarks and gluons and properties of quantum chromodynamics, *Phys. Lett. B* **666**, 95 (2008) [[arXiv:0806.1535](#) [[hep-th](#)]].
- [18] A. Deur, S. J. Brodsky and G. F. de Teramond, Connecting the hadron mass scale to the fundamental mass scale of quantum chromodynamics, *Phys. Lett. B* **750**, 528 (2015) [[arXiv:1409.5488](#) [[hep-ph](#)]].
- [19] S. J. Brodsky, G. F. de Teramond, H. G. Dosch and J. Erlich, Light-front holographic QCD and emerging confinement, *Phys. Rept.* **584**, 1 (2015) [[arXiv:1407.8131](#) [[hep-ph](#)]].
- [20] G. F. de Teramond and S. J. Brodsky, Light-front holography: a first approximation to QCD, *Phys. Rev. Lett.* **102**, 081601 (2009) [[arXiv:0809.4899](#) [[hep-ph](#)]].
- [21] G. F. de Teramond, H. G. Dosch and S. J. Brodsky, Kinematical and dynamical aspects of higher-spin bound-state equations in holographic QCD, *Phys. Rev. D* **87**, 075005 (2013) [[arXiv:1301.1651](#) [[hep-ph](#)]].
- [22] Light-front holographic methods were introduced by matching the electromagnetic form factor in AdS space with the corresponding light-front expression in physical space-time. See: S. J. Brodsky and G. F. de Teramond, Hadronic spectra and light-front wave functions in holographic QCD, *Phys. Rev. Lett.* **96**, 201601 (2006) [[arXiv:hep-ph/0602252](#)].
- [23] J. D. Bjorken, Applications of the chiral $U(6) \otimes U(6)$ algebra of current densities, *Phys. Rev.* **148**, 1467 (1966); Inelastic scattering of polarized leptons from polarized nucleons, *Phys. Rev. D* **1**, 1376 (1970).
- [24] A. Deur, V. Burkert, J. P. Chen and W. Korsch, Experimental determination of the effective strong coupling constant, *Phys. Lett. B* **650**, 244 (2007) [[arXiv:hep-ph/0509113](#)]; Determination of the effective strong coupling constant

- $\alpha_{s,g_1}(Q^2)$ from CLAS spin structure function data, *Phys. Lett. B* **665**, 349 (2008) [[arXiv:0803.4119 \[hep-ph\]](#)].
- [25] V. de Alfaro, S. Fubini and G. Furlan, Conformal invariance in quantum mechanics, *Nuovo Cim. A* **34**, 569 (1976).
 - [26] S. J. Brodsky, G. F. de Teramond and H. G. Dosch, Threefold complementary approach to holographic QCD, *Phys. Lett. B* **729**, 3 (2014) [[arXiv:1302.4105 \[hep-th\]](#)].
 - [27] V. P. Akulov and A. I. Pashnev, Quantum superconformal model in (1,2) space, *Theor. Math. Phys.* **56**, 862 (1983) [*Teor. Mat. Fiz.* **56**, 344 (1983)].
 - [28] S. Fubini and E. Rabinovici, Superconformal quantum mechanics, *Nucl. Phys. B* **245**, 17 (1984).
 - [29] G. F. de Teramond, H. G. Dosch and S. J. Brodsky, Baryon spectrum from superconformal quantum mechanics and its light-front holographic embedding, *Phys. Rev. D* **91**, 045040 (2015) [[arXiv:1411.5243 \[hep-ph\]](#)].
 - [30] H. G. Dosch, G. F. de Teramond and S. J. Brodsky, Superconformal baryon-meson symmetry and light-front holographic QCD, *Phys. Rev. D* **91**, 085016 (2015) [[arXiv:1501.00959 \[hep-th\]](#)].
 - [31] H. G. Dosch, G. F. de Teramond and S. J. Brodsky, Supersymmetry across the light and heavy-light hadronic spectrum, *Phys. Rev. D* **92**, 074010 (2015) [[arXiv:1504.05112 \[hep-ph\]](#)].
 - [32] V. N. Gribov and L. N. Lipatov, Deep inelastic $e p$ scattering in perturbation theory, *Sov. J. Nucl. Phys.* **15**, 438 (1972) [*Yad. Fiz.* **15**, 781 (1972)]; G. Altarelli and G. Parisi, Asymptotic freedom in parton language, *Nucl. Phys. B* **126**, 298 (1977); Y. L. Dokshitzer, Calculation of the structure functions for deep inelastic scattering and e^+e^- annihilation by perturbation theory in quantum chromodynamics, *Sov. Phys. JETP* **46**, 641 (1977) [*Zh. Eksp. Teor. Fiz.* **73**, 1216 (1977)].
 - [33] G. P. Lepage and S. J. Brodsky, Exclusive processes in quantum chromodynamics: Evolution equations for hadronic wave functions and the form factors of mesons, *Phys. Lett. B* **87**, 359 (1979); G. P. Lepage and S. J. Brodsky, Exclusive processes in perturbative quantum chromodynamics, *Phys. Rev. D* **22**, 2157 (1980); A. V. Efremov and A. V. Radyushkin, Factorization and asymptotic behavior of pion form

- factor in QCD, *Phys. Lett. B* **94**, 245 (1980); Asymptotic behavior of the pion electromagnetic form factor in quantum chromodynamics, *Theor. Math. Phys.* **42**, 97 (1980) [*Teor. Mat. Fiz.* **42**, 147 (1980)].
- [34] M. Gell-Mann and F. E. Low, Quantum electrodynamics at small distances, *Phys. Rev.* **95**, 1300 (1954).
 - [35] E. D. Bloom and F. J. Gilman, Scaling, duality, and the behavior of resonances in inelastic electron-proton scattering, *Phys. Rev. Lett.* **25**, 1140 (1970); Scaling and the behavior of nucleon resonances in inelastic electron-nucleon scattering, *Phys. Rev. D* **4**, 2901 (1971).
 - [36] W. Melnitchouk, R. Ent and C. Keppel, Quark-hadron duality in electron scattering, *Phys. Rept.* **406**, 127 (2005) [[arXiv:hep-ph/0501217](#)].
 - [37] K. A. Olive *et al.* [Particle Data Group Collaboration], Review of particle physics, *Chin. Phys. C* **38**, 090001 (2014).
 - [38] See *e.g.*, A. Vairo, A low-energy determination of α_s at three loops, [arXiv:1512.07571 \[hep-ph\]](#).
 - [39] K. G. Chetyrkin, B. A. Kniehl and M. Steinhauser, Strong coupling constant with flavor thresholds at four loops in the modified minimal-subtraction scheme *Phys. Rev. Lett.* **79**, 2184 (1997) [[arXiv:hep-ph/9706430](#)].
 - [40] D. J. Gross and F. Wilczek, Ultraviolet behavior of nonabelian gauge theories, *Phys. Rev. Lett.* **30**, 1343 (1973); H. D. Politzer, Reliable perturbative results for strong interactions?, *Phys. Rev. Lett.* **30**, 1346 (1973); W. E. Caswell, Asymptotic behavior of non-abelian gauge theories to two-loop order, *Phys. Rev. Lett.* **33**, 244 (1974); D. R. T. Jones, Two-loop diagrams in Yang-Mills theory, *Nucl. Phys. B* **75**, 531 (1974); E. Egorian and O. V. Tarasov, Two-loop renormalization of the QCD in an arbitrary gauge, *Teor. Mat. Fiz.* **41**, 26 (1979) [*Theor. Math. Phys.* **41**, 863 (1979)]; O. V. Tarasov, A. A. Vladimirov and A. Y. Zharkov, The Gell-Mann-Low function of QCD in the three-loop approximation, *Phys. Lett. B* **93**, 429 (1980); S. A. Larin and J. A. M. Vermaseren, The three-loop QCD β -function and anomalous dimensions, *Phys. Lett. B* **303**, 334 (1993) [[arXiv:hep-ph/9302208](#)]; T. van Ritbergen, J. A. M. Vermaseren and S. A. Larin, The four-loop β -function in quantum chromodynamics, *Phys. Lett. B* **400**, 379 (1997) [[arXiv:hep-ph/9701390](#)].

- [41] K. G. Chetyrkin and A. Retey, Three-loop three-linear vertices and four-loop MOM beta functions in massless QCD, [arXiv:hep-ph/0007088](#); P. Boucaud, F. De Soto, J. P. Leroy, A. Le Yaouanc, J. Micheli, O. Pene and J. Rodriguez-Quintero, Ghost-gluon running coupling, power corrections, and the determination of $\Lambda_{\overline{MS}}$, *Phys. Rev. D* **79**, 014508 (2009) [[arXiv:0811.2059 \[hep-ph\]](#)]; B. Blossier *et al.* [ETM Collaboration], Ghost-gluon coupling, power corrections and $\Lambda_{\overline{MS}}$ from twisted-mass lattice QCD at $N_f = 2$, *Phys. Rev. D* **82**, 034510 (2010) [[arXiv:1005.5290 \[hep-lat\]](#)].
- [42] J. A. Gracey, Renormalization group functions of QCD in the minimal MOM scheme, *J. Phys. A* **46**, 225403 (2013) [[arXiv:1304.5347 \[hep-ph\]](#)].
- [43] M. Peter, The static potential in QCD – a full two-loop calculation, *Nucl. Phys. B* **501**, 471 (1997) [[arXiv:hep-ph/9702245](#)]; A. L. Kataev and V. S. Molokoedov, Fourth-order QCD renormalization group quantities in the V scheme and the relation of the β function to the Gell-Mann–Low function in QED, *Phys. Rev. D* **92**, 054008 (2015) [[arXiv:1507.03547 \[hep-ph\]](#)].
- [44] J. M. Cornwall and J. Papavassiliou, Gauge-invariant three-gluon vertex in QCD, *Phys. Rev. D* **40**, 3474 (1989).
- [45] J. D. Gomez and A. A. Natale, $R_{e^+e^-}$ and an effective QCD charge, *Phys. Rev. D* **93**, 014027 (2016) [[arXiv:1509.04798 \[hep-ph\]](#)].
- [46] D. Binosi and J. Papavassiliou, Pinch technique: Theory and applications, *Phys. Rept.* **479**, 1 (2009) [[arXiv:0909.2536 \[hep-ph\]](#)].
- [47] A. C. Aguilar, D. Binosi, J. Papavassiliou and J. Rodriguez-Quintero, Non-perturbative comparison of QCD effective charges, *Phys. Rev. D* **80**, 085018 (2009) [[arXiv:0906.2633 \[hep-ph\]](#)]; M. Binger and S. J. Brodsky, Form factors of the gauge-invariant three-gluon vertex, *Phys. Rev. D* **74**, 054016 (2006) [[arXiv:hep-ph/0602199](#)].
- [48] J. A. Gracey, Two loop QCD vertices at the symmetric point, *Phys. Rev. D* **84**, 085011 (2011) [[arXiv:1108.4806 \[hep-ph\]](#)]; Momentum subtraction and the R ratio, *Phys. Rev. D* **90**, 094026 (2014) [[arXiv:1410.6715 \[hep-ph\]](#)].
- [49] N. Isgur and J. E. Paton, A flux-tube model for hadrons in QCD, *Phys. Rev. D* **31**, 2910 (1985).

- [50] J. D. Bjorken, S. J. Brodsky and A. S. Goldhaber, Possible multiparticle ridge-like correlations in very high multiplicity proton-proton collisions, [Phys. Lett. B **726**, 344 \(2013\) \[arXiv:1308.1435 \[hep-ph\]\]](#).
- [51] X. G. Wu, S. J. Brodsky and M. Mojaza, The renormalization scale-setting problem in QCD, [Prog. Part. Nucl. Phys. **72**, 44 \(2013\) \[arXiv:1302.0599 \[hep-ph\]\]](#).